CELL BIOLOGY

A liquid phase of synapsin and lipid vesicles

Dragomir Milovanovic, Yumei Wu, Xin Bian, Pietro De Camilli*

Neurotransmitter-containing synaptic vesicles (SVs) form tight clusters at synapses. These clusters act as a reservoir from which SVs are drawn for exocytosis during sustained activity. Several components associated with SVs that are likely to help form such clusters have been reported, including synapsin. Here we found that synapsin can form a distinct liquid phase in an aqueous environment. Other scaffolding proteins could coassemble into this condensate but were not necessary for its formation. Importantly, the synapsin phase could capture small lipid vesicles. The synapsin phase rapidly disassembled upon phosphorylation by calcium/calmodulin-dependent protein kinase II, mimicking the dispersion of synapsin 1 that occurs at presynaptic sites upon stimulation. Thus, principles of liquid-liquid phase separation may apply to the clustering of SVs at synapses.

The presence of synaptic vesicle (SV) clusters is a defining feature of nerve terminals. SVs are tightly packed in these structures, which are well distinguished from the surrounding cytoplasm, although there is no evidence for a restraining boundary (*1*). Vesicles intermix within the clusters (*2*) and can be exchanged between them (*3*). Although SV clusters present at synapses are anchored to active zones of secretion, active-zone proteins are not required for their formation (*4*, *5*) and small clusters also occur in developing axons before synapse formation (*6*). How the motility of SVs within clusters is compatible with their spatial confinement remains unknown. Recently, liquid-liquid phase separation has been shown to be a mechanism through which components of the cytoplasm (proteins and RNAs) can assemble into distinct compartments (biomolecular condensates) not delimited by a membrane (*7*–*9*). A key feature of proteins that can undergo liquid-liquid phase separation is their ability to engage in multivalent, low-affinity interactions, either through intrinsically disordered regions (IDRs) (*10*, *11*) or through association with binding partners (*8*, *12*). A major constituent of the matrix that connects SVs is synapsin (*13*–*15*), whose abundance in nerve terminals is severalfold higher than the abundance of any other protein specifically localized in this matrix (*16*). Synapsin comprises an adenosine triphosphate (ATP)–binding module of unclear physiological function (*15*, *17*), flanked by an N-terminal short region that partially penetrates membranes (*18*) and a C-terminal IDR (*15*) with multiple SRC homology 3 (SH3) domain–binding motifs (*19*, *20*) (fig. S1). This prompted us to hypothesize (*1*) that synapsin may be a key constituent of a biomolecular condensate that includes SVs.

Departments of Neuroscience and Cell Biology, Howard Hughes Medical Institute, Kavli Institute for Neuroscience, Program in Cellular Neuroscience, Neurodegeneration and Repair, Yale University School of Medicine, New Haven, CT, USA.
*Corresponding author. Email: pietro.decamilli@yale.edu

To assess whether synapsin, which forms homo- and heterodimers, can phase-separate through interactions of its IDR, we incubated enhanced green fluorescent protein (EGFP)–tagged synapsin 1 in a buffer of physiological salt concentration and pH on a glass-bottom dish at room temperature (see methods). After a lag time of tens of minutes, synapsin 1 alone formed micrometer-sized droplets (Fig. 1, A and B; fig. S4; and movie S1), with the size of the droplets correlating with its concentration (0.5 to 20 μM concentrations tested) (figs. S2 and S3). The coalescence of synapsin 1 into droplets was confirmed by performing the incubation in suspension and measuring turbidity (fig. S4). These concentrations were not above the physiological range, as synapsin 1 is estimated to reach concentrations above 100 μM in nerve terminals (*16*). Droplets of synapsin 1 had the expected properties of a liquid phase (*9*): They fused with each other (Fig. 1B), and bleaching of several droplets revealed that synapsin 1 molecules swiftly exchanged into and out of synapsin 1 droplets [half-time ($t_{1/2}$) = 65 s; Fig. 1C and movie S2]. Additionally, fluorescence recovery after photobleaching (FRAP) of a small area within the droplet was followed by rapid recovery ($t_{1/2}$ = 40 s) of fluorescence, reflecting local rearrangement of synapsin 1 molecules (Fig. 1D and movie S3). Analysis of two purified fragments of synapsin 1 confirmed that its IDR (amino acids 421 to 706), but not its folded central ATP-binding module (amino acids 113 to 420), which is known to dimerize (*17*), formed droplets (fig. S1B). Droplet formation by the IDR alone was as efficient as droplet formation by the full-length protein (fig. S5). Synapsin 2, a paralog of synapsin 1 that can heterodimerize with synapsin 1 (*15*, *17*), also contains a C-terminal IDR, albeit shorter than the IDR of synapsin 1. Accordingly, synapsin 2 also phase-separated (fig. S6). Increasing the salt concentration above the physiological range impaired droplet formation, implicating charge-dependent interactions in their formation (fig. S7).

Polyvalent interactions between SH3 domain–containing proteins and proteins harboring cognate proline-rich motifs can also generate distinct liquid phases (*8*, *12*). Synapsin 1 interacts with several SH3 domain–containing proteins via its IDR (*19*–*22*). One such protein, intersectin, is a component of a network of protein-protein interactions that facilitates the clustering of SVs in conjunction with synapsin (*22*, *23*). Thus, we examined whether, upon incubation with SH3 domain–containing binding partners such as intersectin (*22*) and growth factor receptor–bound 2 (GRB2) (*19*), synapsin 1 phase-separated together with them. GRB2 and intersectin contain two and five SH3 domains, respectively (*22*).

Synapsin 1 was mixed with either GRB2 (Fig. 2A and movie S4) or a fragment from human intersectin comprising its five SH3 domains [$(SH3)_{5\text{-intersectin}}$] (Fig. 2B and movie S5) (*21*) (all proteins at 10 μM and fused to fluorescent proteins) and incubated at room temperature in physiological salt concentration. After some delay, droplets appeared containing both synapsin and its binding partners (Fig. 2, A and B, and movies S4 and S5). Droplet growth, after the initial nucleation, was faster than with synapsin 1 alone (fig. S4). As before, droplets grew progressively or by fusing with each other, revealing a liquid state. The same concentration (10 μM) was used for synapsin 1 and

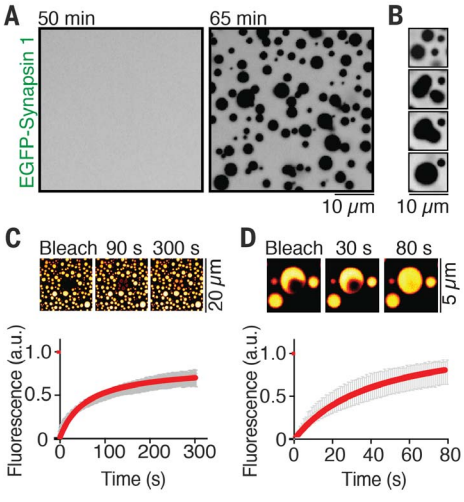

Fig. 1. Synapsin 1 undergoes liquid-liquid phase separation. (**A**) EGFP–synapsin 1 (10 μM) forms droplets when incubated for 1 hour in a buffer of physiological salt concentration at room temperature. (**B**) Droplets of synapsin 1 show liquid behavior by fusing with each other and relaxing into a round-shaped structure, minimizing surface tension. (**C**) Photobleaching of several synapsin 1 droplets with subsequent recovery of fluorescence, as shown by micrograph and by quantification of the fluorescence recovery in the bleached region. (**D**) Fluorescence recovery of synapsin 1 after photobleaching a region within a droplet. Error bars represent SEM, and red shading is the fit with a hyperbolic function. a.u., arbitrary units.

its partners, although synapsin is thought to be the most abundant matrix protein within SV clusters (*16*). This was meant to reflect the presence at synapses of multiple SH3 domain–containing synapsin 1 ligands, and thus a higher collective concentration of these proteins than the concentration of any one of them. The synapsin 1:$(SH3)_{5\text{-intersectin}}$ droplets were larger, which could be explained by the higher valence of the intersectin fragment (five SH3 domains, although with different affinities for synapsin) relative to GRB2 (two SH3 domains) (*22*, *24*).

The cytoplasm of a synaptic bouton is a crowded environment filled with organelles and macromolecules. To mimic this environment in subsequent experiments, we added polyethylene glycol (PEG), a crowding reagent, to the buffer. In the presence of 3% PEG 8000, droplets of synapsin 1 alone (fig. S3) or of synapsin 1 and its binding partners (Fig. 2, C and D) formed immediately, with no lag phase. FRAP confirmed that, even under these conditions, proteins were mobile within the droplets, with a faster recovery time for synapsin 1 in droplets generated with GRB2 ($t_{1/2}$ at 1.5 min) than in those generated with $(SH3)_{5\text{-intersectin}}$ ($t_{1/2}$ at 3.2 min) (Fig. 2, E and F). This, again, possibly reflects the higher valence of this protein relative to GRB2. Recovery of fluorescence was observed both when a region within a droplet (Fig. 2, E and F) and when the entire droplet was bleached (fig. S8), indicating that recovery results from both molecular rearrangements within the droplet and the exchange of molecules with the dilute phase. Presence of a synapsin 1 binding partner, $(SH3)_{5\text{-intersectin}}$, had a biphasic effect on droplet formation. It enhanced this process at low-to-moderate excess stoichiometric ratio but inhibited it when added in large excess (fig. S9). Thus, $(SH3)_{5\text{-intersectin}}$ is not only a "client" of synapsin but also an active player in the formation of the liquid condensate. The negative effect at high stoichiometric ratio may be due to the masking of sites within the synapsin IDR that interact with each other. Recruitment of synapsin interactors into the droplets was specific and did not occur with proteins that do not bind synapsin (fig. S10).

Synapsin binds SVs (*15*, *18*, *25*). If its phase-separating properties are involved in SV cluster formation, synapsin 1 should be capable of capturing vesicles into such a phase. We thus incubated synapsin 1 with small lipid vesicles (~50 to 150 nm in diameter) mimicking SVs in lipid composition supplemented with a fluorescently labeled lipid, 1,2-dioleoyl-*sn*-glycero-3-phosphoethanolamine-*N*-(cyanine 5) (DOPE-Cy5). Formation of synapsin droplets correlated with the appearance of droplets positive for the labeled lipid, whereas no droplets positive for the lipid were observed in the absence of synapsin 1 (Fig. 3A). Synapsin 1 condensates did not recruit vesicles lacking negatively charged phospholipids (fig. S11), which is expected, given that negatively charged lipids are necessary for synapsin binding to vesicles (*26*). Other well-characterized protein liquid condensates that do not bind lipid membranes, such as droplets composed of cytoplasmic protein noncatalytic region of tyrosine kinase adaptor protein 1 (NCK) and a fragment of neural Wiskott-Aldrich syndrome protein (N-WASP) that does not include the phospholipid-binding region (*8*), did not sequester lipid vesicles (fig. S12). Lipid vesicles were mobile within the synapsin phase, as indicated by FRAP (fig. S13). Furthermore, lipid vesicles and SH3-domain synapsin 1 interactors coassembled with synapsin (fig. S14). Electron microscopy (EM) analysis showed that these droplets were represented by clusters of small vesicles, whereas in the absence of synapsin 1, vesicles remained dispersed (Fig. 3, B and C).

Synapsin 1 is a major presynaptic phosphoprotein that undergoes multisite phosphorylation (*14*). Sustained nerve-terminal stimulation to trigger massive neurotransmitter release also induces the calcium-dependent phosphorylation

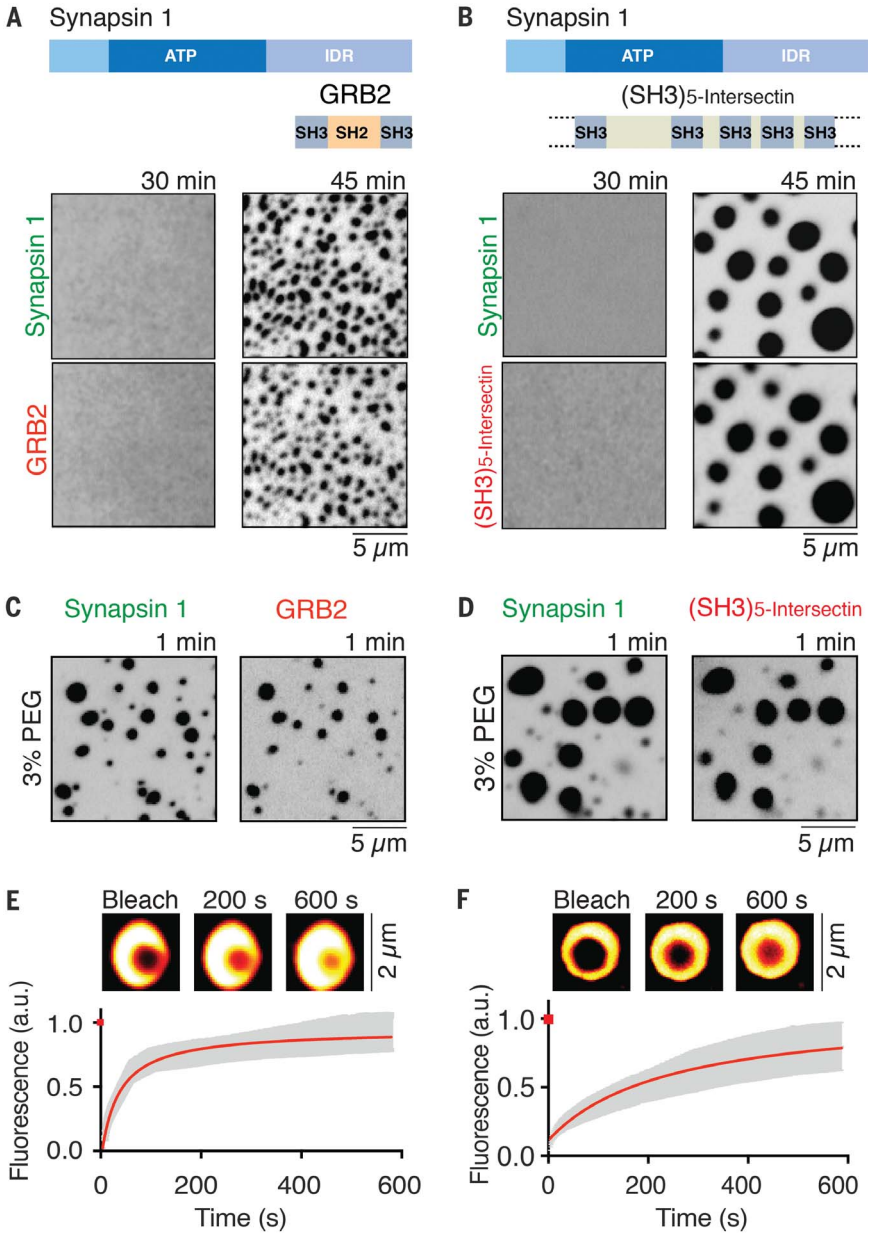

Fig. 2. Synapsin 1 drives phase separation of SH3 domain–containing binding partners. (**A** and **B**) Full-length synapsin 1 (10 μM) and either GRB2 (10 μM) (A) or the SH3 domain–containing region of intersectin (10 μM) (B) form droplets under physiological conditions. The domain organization of the proteins is shown at the top, and fluorescence images of the protein mixtures at 30 and 45 min are shown at the bottom. (**C** and **D**) Fluorescence images of the solution immediately (within 1 min) after mixing of synapsin 1 with GRB2 (C) or $(SH3)_{5\text{-intersectin}}$ (D) in the presence of the crowding reagent (3% PEG 8000). (**E** and **F**) Fluorescence recovery of synapsin 1 after photobleaching a region within a synapsin 1–GRB2 droplet (E) or a synapsin 1–$(SH3)_{5\text{-intersectin}}$ droplet (F). Error bars represent SEM, and red shading is the fit with a hyperbolic function.

of synapsin 1 (*27*). This results in its dissociation from SVs and dispersion within the nerve-terminal cytosol (*28*, *29*), as SVs are consumed by exocytosis. If the formation of a biomolecular condensate by synapsin has a physiological importance in its coassembly with SVs, one would expect synapsin 1 droplets to disassemble upon calcium-dependent phosphorylation. Two prominent phosphorylation sites for calcium/calmodulin-dependent protein kinase II (CaMKII), called sites 2 and 3, are present in its IDR (*14*, *15*). Addition of CaMKII, calcium, and calmodulin to synapsin 1–containing samples did not disperse droplets. Indeed, CaMKII, which binds synapsin 1 (*29*), was recruited into the droplets

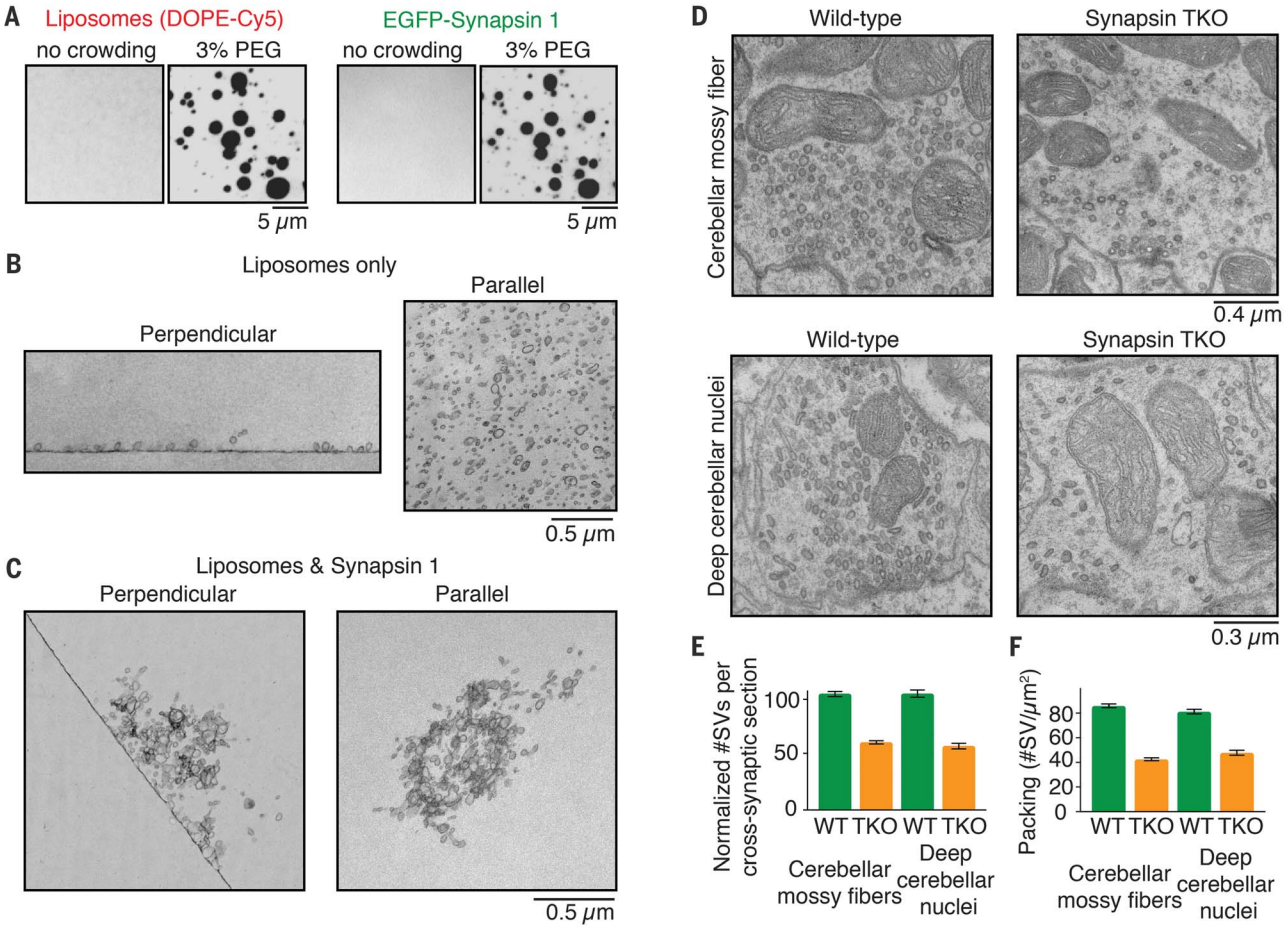

Fig. 3. Synapsin 1 condensates are reaction centers that are able to sequester lipid vesicles. (**A**) Fluorescence images showing the detection of liposomes (left, DOPE-Cy5) and synapsin 1 (right, EGFP–synapsin 1) in a mixture of liposomes and synapsin 1 either without or with crowding agent (3% PEG 8000). (**B**) EM images of liposomes incubated without synapsin 1 in the same buffer conditions used for (A). Left panel shows section perpendicular to the liposome-glass interface. Right panel shows section comprising the layer of liposomes adsorbed to the glass surface. (**C**) Same as in (B), but showing liposomes incubated with synapsin 1. The field shown at right is from a section parallel to the glass surface but above the glass interface. (**D**) EM images of synapses from cerebellar mossy fibers (top) and deep cerebellar nuclei (bottom) obtained from adult wild-type (WT, left) and synapsin triple-knockout (TKO, right) mice. (**E**) Number of SVs in synaptic cross sections of WT and synapsin TKO mice, normalized to WT. (**F**) Number of SVs per unit area of synaptic section in WT and synapsin TKO mice. For each condition, 50 sections from three independent animals were examined. Error bars represent SEM.

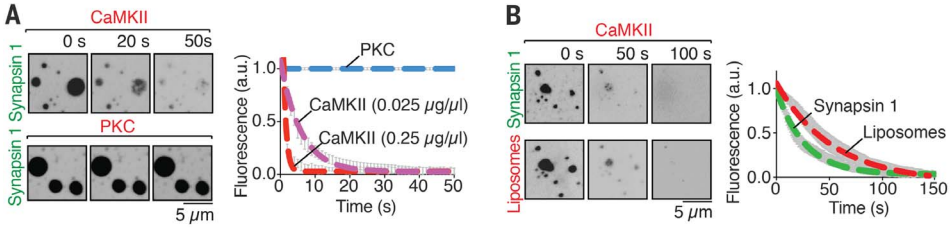

Fig. 4. Phosphorylation of the IDR of synapsin 1 disperses condensates of either synapsin 1 alone or synapsin 1 and liposomes. (**A**) Left panel shows fluorescence images of EGFP–synapsin 1 condensates preincubated with either CaMKII (0.025 μg/μl), calmodulin, and calcium or protein kinase C (PKC), phosphatidylserine, diacylglycerol, and calcium upon addition of ATP (200 μM) at 0 s, demonstrating dispersion of synapsin by CaMKII but not by PKC. Right panel shows time course of the effect of the kinases on the condensates, as assessed by the decrease of fluorescence on regions of interest corresponding to randomly selected droplets. (**B**) Left panel shows fluorescence images of liposome-synapsin condensates preincubated with CaMKII (0.25 μg/μl), calmodulin, and calcium upon addition of ATP (200 μM) at 0 s, demonstrating dispersion of both synapsin and liposomes. Right panel shows time course of the effect of CaMKII on liposome-synapsin droplets dispersion. Error bars represent SEM, and dashed lines represent the fit with a single exponential function. Incubations were carried out at room temperature in a buffer of physiological salt concentration supplemented with 3% PEG 8000.

(Fig. 4A). However, further addition of ATP (200 μM) to induce synapsin 1 phosphorylation caused rapid dispersal of both synapsin 1 and CaMKII [mean lifetime (τ) of 5.9 s] (Fig. 4A, fig. S15, and movie S6). Importantly, CaMKII also disassembled synapsin 1–liposome droplets (Fig. 4B and movie S7). As a control, we added protein kinase C to the droplets, for which synapsin 1 is not a substrate (*30*), but neither addition of the kinase nor the subsequent addition of ATP (200 μM) affected the droplets (Fig. 4A). The lack of effect of ATP in the latter experiment also rules out that droplet dispersion may be explained by a hydrotrope action of this nucleotide (*31*). Such an action, as reported for liquid droplets generated by other proteins, occurs only at much higher ATP concentrations (fig. S16) than the one used in our phosphorylation assay (see also fig. S4).

Strong evidence points to a physiological master role of synapsin in the clustering of SVs at living synapses (*25*, *32*–*34*). In neuronal cultures from mice that lack all three synapsins, the number of SVs at synapses is lower than that in wild-type mice, and this decrease is selective for SVs away from active zones (*33*). We extended these results. Even at synapses in situ—both excitatory (cerebellar mossy fibers) and inhibitory (deep cerebellar nuclei) nerve terminals—not only the total number but also the packing of SVs was notably lower in synapsin triple-knockout mice than in wild-type mice (Fig. 3, D to F).

Collectively, these findings demonstrate that synapsin can form a separate liquid biomolecular condensate either alone or together with binding partners for its IDR, with lipid vesicles, or with both. Interactions occurring at the presynapse in situ are expected to be more complex than the interactions of synapsin with the two SH3 domain–containing proteins and artificial lipid membranes described here. Because SVs are membranous organelles selectively recruited into clusters, there must be additional factors that help provide specificity. However, the minimal systems used here provide some insight into the mechanisms responsible for the properties of SV clusters. Clusters of other membranous organelles may self-organize according to similar principles without the need for a surrounding membrane or protein-based structure to confine them.

REFERENCES AND NOTES

1. D. Milovanovic, P. De Camilli, *Neuron* **93**, 995–1002 (2017).
2. S. O. Rizzoli, W. J. Betz, *Science* **303**, 2037–2039 (2004).
3. K. J. Darcy, K. Staras, L. M. Collinson, Y. Goda, *Nat. Neurosci.* **9**, 315–321 (2006).
4. C. Acuna, X. Liu, T. C. Südhof, *Neuron* **91**, 792–807 (2016).
5. S. S. H. Wang *et al.*, *Neuron* **91**, 777–791 (2016).
6. K. Kraszewski *et al.*, *J. Neurosci.* **15**, 4328–4342 (1995).
7. C. P. Brangwynne *et al.*, *Science* **324**, 1729–1732 (2009).
8. P. Li *et al.*, *Nature* **483**, 336–340 (2012).
9. S. F. Banani, H. O. Lee, A. A. Hyman, M. K. Rosen, *Nat. Rev. Mol. Cell Biol.* **18**, 285–298 (2017).
10. A. Patel *et al.*, *Cell* **162**, 1066–1077 (2015).
11. J. B. Woodruff *et al.*, *Cell* **169**, 1066–1077.e10 (2017).
12. S. F. Banani *et al.*, *Cell* **166**, 651–663 (2016).
13. P. De Camilli, S. M. Harris Jr., W. B. Huttner, P. Greengard, *J. Cell Biol.* **96**, 1355–1373 (1983).
14. W. B. Huttner, W. Schiebler, P. Greengard, P. De Camilli, *J. Cell Biol.* **96**, 1374–1388 (1983).
15. T. C. Südhof *et al.*, *Science* **245**, 1474–1480 (1989).
16. B. G. Wilhelm *et al.*, *Science* **344**, 1023–1028 (2014).
17. M. Hosaka, T. C. Südhof, *J. Biol. Chem.* **274**, 16747–16753 (1999).
18. F. Benfenati, M. Bähler, R. Jahn, P. Greengard, *J. Cell Biol.* **108**, 1863–1872 (1989).
19. P. S. McPherson *et al.*, *Proc. Natl. Acad. Sci. U.S.A.* **91**, 6486–6490 (1994).
20. F. Onofri *et al.*, *J. Biol. Chem.* **275**, 29857–29867 (2000).
21. M. Yamabhai *et al.*, *J. Biol. Chem.* **273**, 31401–31407 (1998).
22. F. Gerth *et al.*, *Proc. Natl. Acad. Sci. U.S.A.* **114**, 12057–12062 (2017).
23. Å. M. E. Winther *et al.*, *J. Neurosci.* **35**, 14756–14770 (2015).
24. A. Pechstein *et al.*, *EMBO Rep.* **16**, 232–239 (2015).
25. P. De Camilli, F. Benfenati, F. Valtorta, P. Greengard, *Annu. Rev. Cell Biol.* **6**, 433–460 (1990).
26. F. Benfenati, P. Greengard, J. Brunner, M. Bähler, *J. Cell Biol.* **108**, 1851–1862 (1989).
27. W. B. Huttner, L. J. DeGennaro, P. Greengard, *J. Biol. Chem.* **256**, 1482–1488 (1981).
28. P. Chi, P. Greengard, T. A. Ryan, *Nat. Neurosci.* **4**, 1187–1193 (2001).
29. F. Benfenati *et al.*, *Nature* **359**, 417–420 (1992).
30. J. K. Wang, S. I. Walaas, P. Greengard, *J. Neurosci.* **8**, 281–288 (1988).
31. A. Patel *et al.*, *Science* **356**, 753–756 (2017).
32. V. A. Pieribone *et al.*, *Nature* **375**, 493–497 (1995).
33. D. Gitler *et al.*, *J. Neurosci.* **24**, 11368–11380 (2004).
34. L. Siksou *et al.*, *J. Neurosci.* **27**, 6868–6877 (2007).

ACKNOWLEDGMENTS

We thank A. C. Nairn for providing CaMKII and for discussion and the HHMI Summer Institute at the Marine Biology Laboratory for providing NCK and N-WASP. **Funding:** P.D.C. was supported by grants from the NIH (R37NS036251 and DA018343), and D.M. and X.B. were supported by a long-term postdoctoral fellowship from the Human Frontier Science Program. **Author contributions:** D.M. and P.D.C. designed the research and wrote the paper. D.M. designed and performed all of the imaging studies, FRAP and phosphorylation experiments, and liposome clustering. Y.W. performed EM analysis. X.B. helped with protein preparation. **Competing interests:** The authors declare no competing interests. **Data and materials availability:** All data are available in the main text or the supplementary materials.

SUPPLEMENTARY MATERIALS

www.sciencemag.org/content/361/6402/604/suppl/DC1
Materials and Methods
Figs. S1 to S16
Table S1
References (*35*–*38*)
Movies S1 to S7

13 March 2018; accepted 25 June 2018
Published online 5 July 2018
10.1126/science.aat5671

A liquid phase of synapsin and lipid vesicles

Dragomir Milovanovic, Yumei Wu, Xin Bian and Pietro De Camilli

Science **361** (6402), 604-607.
DOI: 10.1126/science.aat5671originally published online July 5, 2018

Going through a phase

Neuronal communication at synapses relies on regulated neurotransmitter secretion. Neurotransmitters are stored in small vesicles that are organized in clusters within nerve terminals. On stimulation, the vesicles fuse with the presynaptic plasma membrane, but despite their tight packing, replacement synaptic vesicles are rapidly recruited. Vesicles newly reformed by membrane recycling randomly intermix with the clusters. Milovanovic *et al.* show that synapsin, an abundant synaptic vesicle–associated protein, organizes these vesicle clusters by liquid-liquid phase separation—like oil in water.

Science, this issue p. 604